

**hMSCs bridging across micro-patterned grooves**

Journal:	<i>RSC Advances</i>
Manuscript ID:	RA-ART-04-2015-006414.R1
Article Type:	Paper
Date Submitted by the Author:	11-May-2015
Complete List of Authors:	Zhang, Qing; South China university of technology, Li, Yuli; South China university of technology, Sun, Hao; Bruker Nano Surfaces Division, Zeng, Lei; South China university of technology, Li, Xian; South China university of technology, Yuan, Bo; South China university of technology, Ning, Chengyun; South China university of technology, Dong, Hua; South China university of technology, Chen, Xiaofeng; South China university of technology,



## Journal Name

## ARTICLE

## hMSCs bridging across micro-patterned grooves

Qing Zhang<sup>abc</sup>, Yuli Li<sup>abc</sup>, Hao Sun<sup>d</sup>, Lei Zeng<sup>abc</sup>, Xian Li<sup>abc</sup>, Bo Yuan<sup>abc</sup>, Chengyun Ning<sup>abc</sup>, Hua Dong<sup>abc\*</sup>, Xiaofeng Chen<sup>abc\*\*</sup>

Received 00th January 20xx,  
Accepted 00th January 20xx

DOI: 10.1039/x0xx00000x

www.rsc.org/

The effect of topography on hMSCs has been widely investigated in recent years. In this study, hMSCs exhibited complex behavior in addition to “contact guidance” on micro-grooved substrates that contain grooves of dimensions ranging from tens to hundreds of microns. A unique growth pattern that hMSCs spanned across grooves with 100 μm width between adjacent plateaus was demonstrated. hMSCs on the bottom of groove explored their possible adhesion positions and spanned across grooves by climbing side wall of grooves. Besides, hMSCs only bridged across the groove in case that the ratio of groove width to depth is less than two. Furthermore, disorganized parallel actin stress fibers and enhanced actin edge-bundles were obviously revealed by characterization of F-actin. However, according to the results of AFM and immunofluorescence, there was no difference between the bridging hMSCs and normal spreading hMSCs on stiffness, expression of desmin and osteocalcin, respectively. Those results from this study offer more information to understand the interaction between hMSCs and the micron topography, and influence the design of future tissue engineering scaffolds that tailor topographical features so as to optimize cell-scaffold interactions.

## Introduction

Biomaterials have been widely used and researched in clinic and regenerative medicine.<sup>1-4</sup> Especially, the development of 3D printing technology makes it possible to create personalized substrates or implants for patients.<sup>5-7</sup> However, the interaction between biomaterials and cells is little known. Unlike chemistry characters, the effect of which on cell's behaviors has been studied for many years, the relationship between physical properties of biomaterials such as topography, hardness and cell fate has attracted great attention in recent ten years. Surface topography of biomaterials including porous structure, roughness and pattern can influence cells adherence, spreading, migration, proliferation and differentiation. Interestingly, cells can span across holes or grooves on the surface of biomaterials regardless of the chemistry properties of the surface and hang their body in the air.<sup>8-19</sup> This phenomenon has never been observed in traditional 2D culture, but this behavior can be common seen when cell cultured on 3D scaffold or in vivo. This behavior of cells and its influence on cells fate have been less studied and need further explored.

hMSCs have multiple differentiation potential, showing low immunogenicity and are easy to be gained from the same patient.<sup>20, 21</sup> Researchers aim at creating a biomimetic microenvironment to induce directed differentiation of stem cells.<sup>22, 23</sup> Topography, a key factor of microenvironment, can influence hMSCs behaviors from adhesion and migration to differentiation. In this research, an unusual phenomenon is investigated that hMSCs span across grooves with widths up to 100 μm. Under these circumstances, the nature property of hMSCs may be changed. As no work has been done on this behavior of hMSCs, it is essential to have a systematically and deep research on this phenomenon which is very important for implants designing and biomimetic niche creating. To explore this phenomenon, soft lithography techniques and melt-casting method are combined to produce polycaprolactone (PCL) micro-grooved substrates with varying groove widths and depths. The effect of groove width and depth on bridged behavior of hMSCs, the mechanism of how they span across the groove and the influence of bridge behavior on their fate are investigated in this study.

## Experiment

## Substrate fabrication

Micro-grooved PCL substrates were fabricated by a combination of standard soft photolithography and melt-casting techniques. Silicon wafers (from Kaihua Set Crystal Silicon Management Department, <111>) were washed with sulfuric acid and hydrogen peroxide mixture (ratio of 7:3, v/v), followed by a sequential rinsing with

Department of Biomedical Engineering, School of Materials Science and Engineering  
National Engineering Research Center for Tissue Restoration and Reconstruction  
Key Laboratory of Biomedical Materials and Engineering, Ministry of Education  
South China University of Technology, GuangZhou, 510006, P.R. China. E-mail: donghua@scut.edu.cn; chenxf@scut.edu.cn; Tel.: +86 20 39380256; fax: +86 20 22236088  
Bruker Nano Surfaces Division, Bruker (Beijing) Scientific Technology Co.Ltd., Beijing 100081, China

isopropanol, acetone and deionized water. AR Grade sulfuric acid, hydrogen peroxide, isopropanol and acetone were purchased from Guangzhou Chemical Reagent Factory. Deionized water was produced by a water purification system (Millipore S.A.S.). After drying with nitrogen (from Guangzhou Sheng Ying Gas Limited Company, China), a negative photoresist (Futurrex, NR21-20000P, USA) was spin-coated on the cleaned silicon wafers to form a uniform film with the thickness of 25  $\mu\text{m}$ , 50  $\mu\text{m}$  and 100  $\mu\text{m}$ , respectively. Master moulds were produced by transferring photomask (Shenzhen Microcad Photomask LTD, China) patterns to the photoresist according to the manufacturer's protocol. Polydimethylsiloxane (PDMS, Sylgard 184, Dow Corning, Midland) templates with defined topographies were then created by pouring elastomer and curing agent (ratio of 10:1, w/w) over the photoresist master and heating on a hot plate (Shanghai Chamet Function ceramics Technology Limited Company, ModelKw-4AH, China) at 60  $^{\circ}\text{C}$  for 4 hours. PCL (M.W = 60,000, Dai Gang Biology, China) substrates were produced by melting PCL particles on PDMS templates. Prior to use, all PCL samples were sterilized in 75% AR Grade ethanol (Guangzhou Chemical Reagent Factory, China) for 24 h and rinsed by a phosphate buffer solution (PBS).

#### cell culture and seeding

Human mesenchymal stem cells (hMSCs) were purchased from Cyagen Biosciences. hMSCs were cultured in DMEM supplemented with 10% FBS and 1% penicillin/streptomycin antibiotics (all from Cyagen biosciences) at 37  $^{\circ}\text{C}$  and 5%  $\text{CO}_2$  in 75  $\text{cm}^2$  culture flask. Cells were used in the experiment at passage eight.

Sterilized PCL substrates were first placed into a 24-well cell culture plate (Corning, USA). Cells were then suspended in culture media ( $4 \times 10^4$  cells per ml) and seeded onto each PCL surface (1ml / well).

#### Scanning electronic microscopy (SEM) characterization

SEM observations were used to analyze the morphology of the hMSCs cultured on PCL substrates. hMSCs were seeded on PCL substrates as described above. Culture medium was removed at the end of the incubation and cells were rinsed with PBS. The sample were then fixed with 2.5% glutaraldehyde (GuangZhou Chemical Reagent Factory, China) for 12 hours and rinsed with PBS. After twice rinsed with PBS, the samples were then dehydrated in a graded series of ethanol: 5, 70, 80, 90, 95, 100%. After sputtered with platinum the samples were observed under scanning electronic microscope (NOVA NANOSEM 430, Philips, Netherlands).

#### Characterization of Cell cytoskeleton and nuclear

Morphology of hMSCs cultured on PCL substrates was analyzed by a laser scanning confocal microscope (LSCM, Leica SP5, Germany). F-actin and cell nucleus were stained by phalloidin-FITC and DAPI, respectively. After being immersed in a 4% formaldehyde (Guangzhou Chemical Reagent Company, AR Grade, China) solution for 30 min, Cells were permeated with 0.1% Triton X-100 (UNI-Chem, Serbia). They were then incubated with phalloidin-FITC (AAT

Bioquest, USA) and DAPI (Beyotime, C1006, China) sequentially. Images were taken by a laser scanning confocal microscope (LSCM, Leica SP5, Germany) to analyze the cytoskeleton.

#### Counting of hMSCs bridges

Samples plated with cells were examined on Hirox KH-7700 digital microscope. Fixed by a 4% formaldehyde (Guangzhou Chemical Reagent Company, AR Grade, China) solution for 30 min, samples were immersed in a 0.01% Coomassie Brilliant Blue solution (ShangHai LanJi). The number of bridges was counted and compared among different groups (three samples replicates).

#### Cell mechanics analysis by AFM

Cells were cultured on grooved substrates two days, then fixed with 4% paraformaldehyde (Sigma-alorich, USA) and dried in the air. Three samples replicates were for every group. Three cells were chose to test elasticity modulus at least. The test procedure was done in the air.

Dimension Icon AFM (Bruker, Santa Barbara, CA) was used for mechanical properties mapping on cells above both substrates and grooves. Topographic and PeakForce Capture images were collected simultaneously under PeakForce QNM mode at 0.5 Hz scan rate. Commercial silicon nitride probes (Model "Scanasyt-Air", Bruker, Santa Barbara, CA) and Stargate Scanner (max. scan size =  $\sim 100 \mu\text{m}$ ) were used to scan the sample. The deflection sensitivity of the cantilever was calibrated on sapphire and the spring constant was calibrated by thermal tune method. Tip radius was measured on the RS-15M tip check sample (Bruker, Santa Barbara, CA) for Young's modulus calculation with DMT model.

The PeakForce QNM mode is based on Peak Force Tapping (PFT) which performs a very fast force curve at every pixel in the image by modulating the Z piezo at  $\sim 1 \text{ kHz}$  with an amplitude of 300 nm in this study. The peak force of each of these curves was then used as the imaging feedback signal and also used to real time Young's modulus calculation. The force curve at every pixel was recorded in the PeakForce capture (PFC) file.

#### Immunofluorescence of OCN and desmin

After 21 days of culture (three samples replicates), hMSCs were fixed in 4% formaldehyde for 20min at 4  $^{\circ}\text{C}$  and then incubated in 10% FBS in PBS for 20min and blocked non-specific protein-protein interactions. The cells were incubated with the antibody (anti-osteocalcin antibody [OC4-30], ab13418, Abcam, USA, 1/80) overnight at 4  $^{\circ}\text{C}$ . The secondary antibody was Cy3-conjugated affininpure goat anti-mouse IgG (H+L) (SA00009-1, proteintech, USA) used at 1/50 dilution for 1 hour. F-actin and nuclei were labeled by phalloidin-FITC and DAPI as described above. hMSCs cultured in culture plate with osteoblast inducing conditional media were as positive control. hMSCs cultured on plate PCL substrates with normal media were as negative control.

Immunofluorescence of desmin was made by the same way. hMSCs were fixed when they were cultured on the 5th day and 16th day. C2C12 cultured in high sugar DMEM with 5% equinum serum were as positive control. hMSCs cultured on plate PCL substrates with normal media were as negative control.

### Cytochalasin D and Nocodazole treatments of hMSCs

Cytochalasin D and Nocodazole were used to disorganize microfilaments and microtubules of hMSCs respectively. Typically, hMSCs were treated with 0.25  $\mu\text{g}/\text{ml}$  cytochalasin D or 1  $\mu\text{g}/\text{ml}$  nocodazole after seeding on substrates 1 day. After 0.5 h, cells were fixed by a 4% formaldehyde (Guangzhou Chemical Reagent Company, AR Grade, China) solution for 30 min. Then samples were stained by a 0.01% Coomassie Brilliant Blue solution (ShangHai LanJi). Hirox KH-7700 digital microscope was used to observe cells morphology. As control, cells were treated with 0.2% dimethyl sulfoxide (DMSO), which was used as vehicle of the drugs. No differences were observed on cell morphology and cytoskeletal integrity of untreated and DMSO treated cells.

### Statistical Analysis

One-way analysis of variance was used to evaluate the corresponding effect of the groove width and depth on the fracture healing. Two-way analysis of variance was used to evaluate the interactive effect of groove width and depth.

## Result and dicussion

### Micro-grooved substrates

Micro-grooved PCL substrates contain repeating rectangular groove-plateau patterns. Figure 1 shows the SEM image of micro-grooved PCL substrates with 50  $\mu\text{m}$  depths, 25  $\mu\text{m}$  widths grooves and a constant plateau width of 200  $\mu\text{m}$ . Identical, the surfaces of the sample are clean and have no impurity particles. The shape and size of micro-groove are in good accordance with the design. PCL samples are labeled in the following section by a numbering format such as D25W50 (groove depth: 25  $\mu\text{m}$ , groove width: 50  $\mu\text{m}$ ) and D50W100 (groove depth: 50  $\mu\text{m}$ , groove width: 100  $\mu\text{m}$ ). The micro-grooved substrates used in this study include D100W200, D100W100, D100W50, D50W200, D50W100, D50W50, D50W25, D25W200, D25W100, D25W50, D25W25.

Unlike some polymer gel which is very soft and easily changed shape by cells adhesion,<sup>24</sup> the micro-grooved PCL structure is stable and consistent during all experiment process. The surface of living cells is rather soft and delicate and the stiffness of hMSCs was 1.2~3.4 kPa.<sup>25-27</sup> The elastic modulus of PCL is 210~440 MPa<sup>28</sup> and PCL degrades very slowly in vitro in the absence of enzymes and in vivo as well.<sup>29-31</sup> The longest cells culturing period on PCL substrates is 21 days in our study. It did not begin to degrade.

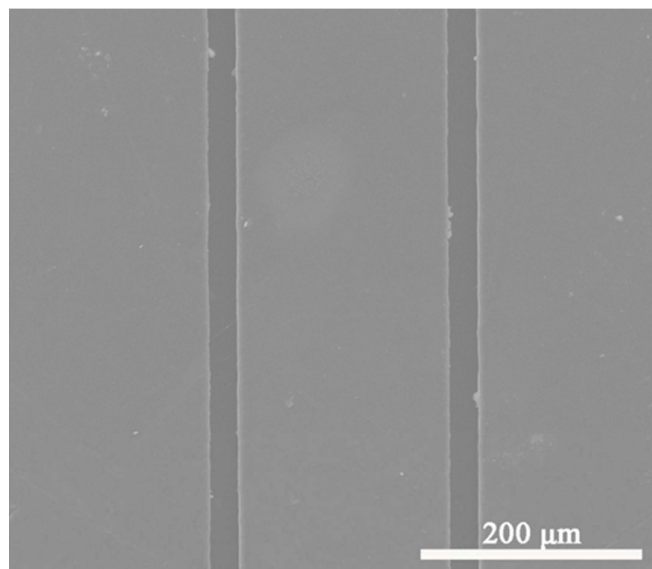


Figure 1. The SEM picture of PCL with 50  $\mu\text{m}$  depths and 25  $\mu\text{m}$  widths grooves, 200 $\mu\text{m}$  widths plateaus.

### bridges across microgrooves

Topographical surface features of substrates can influence behaviors and functions of hMSCs.<sup>32-34</sup> hMSCs show contact guidance when exposed with grooved topographical features at the nanometer to micron scale.<sup>35-37</sup> In present study, accompanying with their ability to align to grooves and plateaus, hMSCs displayed an additional capacity for a distinctly different response. As shown in Fig.2, hMSCs could form "bridge" spanning from one plateau to an adjacent plateau across micro-groove. The widest of groove is 100 $\mu\text{m}$  which hMSCs can span.

In this study, cells hung themselves in the air through variety of ways. According to the position that they contacted with substrates, these bridging phenomena were divided into five categories, as shown in figure 2. Figure 2 A(a) and C(a) show cells contacted with substrate at three different positions: bottom, two adjacent plateaus. The second situation, as shown in Figure 2 A(b) and C(b), cells contacted with substrates at two positions: bottom and plateau or the side wall of groove. Both of the two situations, cells extended between bottom and plateau. The rest of the three conditions, cells hung their body above the bottom and spanned across the whole groove, i.e. cells extended between groove wall and wall (figure 2 A(c) and C(c)), or groove wall and plateau (figure 2 A(d) and C(d)), or two adjacent plateaus (figure 2 A(e) and C(e)). Figure 2 A(f) and C(f) show a cluster of hMSCs spanned across the groove.

As can be seen in table 1 and 2, the number of hMSCs which bridge across groove is increasing with the incubation time, and the fluorescence staining of cytoskeleton and nuclear of the bridges are positive which confirm that the bridges are hMSCs but not impurity substances. The result observed by digital microscope also indicates that the hMSCs bridges exhibited diverse morphologies, as demonstrated by SEM.

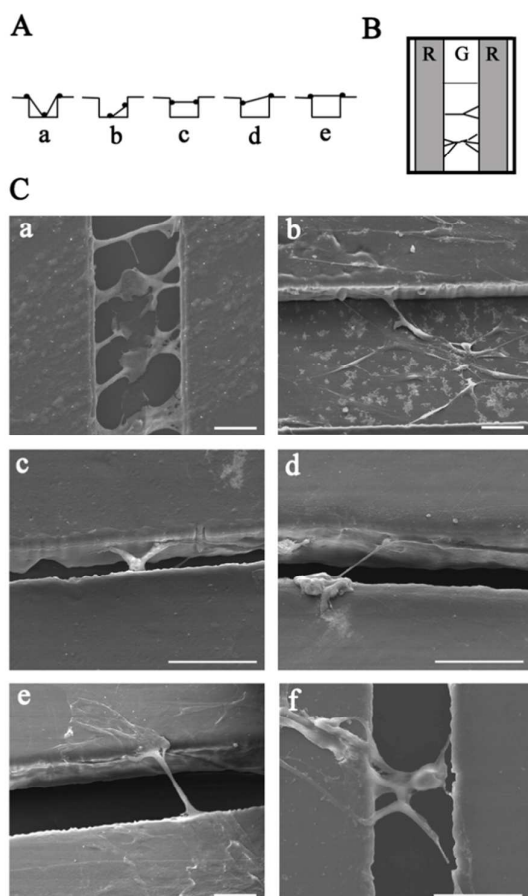


Figure 2. Picture A (sketch maps) and C (photos of SEM) show various ways in which hMSCs extended on micro-grooved topography. A (a) and C (a): cells contacted with substrates at three different positions: bottom, two adjacent plateaus. A (b) and C (b): cells contacted with substrates at two positions: bottom and wall of groove or plateau. A(c) and C(c), A(d) and C(d), A(e) and C(e) severally show hMSCs extended between wall and wall, wall and plateau, or two adjacent plateaus with cell body spanning across a whole groove. A(f) and C(f): a cluster of hMSCs spanned across the groove. B shows all the sketch map of the bridge morphologies viewed from top, each of them is a bridge as the “bridge” definition. Scale bar = 50  $\mu\text{m}$ .

Table 1 the numbers of bridges on different substrates on the first day

Depth/ $\mu\text{m}$ Bridge Width/ $\mu\text{m}$ numbers	D100	D50	D25
W200	0	0	0
W100	5 $\pm$ 1	6.67 $\pm$ 3.21	0
W50	28 $\pm$ 3.64	37.67 $\pm$ 4.62	21.67 $\pm$ 11.68
W25	###	133.67 $\pm$ 23.18	192 $\pm$ 37.24

Table 2 the numbers of bridges on different substrates on the third day

Depth/ $\mu\text{m}$ Bridge Width/ $\mu\text{m}$ numbers	D100	D50	D25
W200	0	0	0
W100	16.33 $\pm$ 6.11	0	0
W50	115 $\pm$ 9.54	127.33 $\pm$ 66.90	0
W25	###	393.75 $\pm$ 128.89	382.75 $\pm$ 139.30

#### Conditions for hMSCs bridges

To explore the conditions for hMSCs bridging across the groove, the numbers of bridges at different time points are compared among different groups which involve series of depth and width of groove. To count objectively, a “bridge” is defined as a cellular bridge which span across a whole groove and hang in the air between two adjacent plateaus (figure 2 A (d) and C (d), A(c) and C(c), A (e) and C (e), A (f) and C (f)). An hMSCs bridge which belongs to one kind of these types of extensions is counted as one bridge. In some cases a bridge was composed of a bunch of cells (figure 2 C (d) and (e)). Others a bridge was composed of a few bunches of cells (figure C (c) and (f)). In some cases a bridge was composed of a single hMSC or multiple hMSCs as revealed by cell nucleus staining. Figure 2B show all the sketch map of the bridge morphologies viewed from top and observed by SEM and digital microscope.

The number of hMSCs bridges is significantly influenced by the groove width ( $p < 0.05$  for groove width of 50  $\mu\text{m}$  and cultured on the third day,  $p < 0.001$  for other experiment groups, One-way analysis of variance) when hMSCs cultured for one day or three days (table 1 and 2). The number of hMSCs bridges is increasing with decreasing of the groove width. However, as for the effect of

groove depth on the numbers of bridges, it can be more complicated than that of groove width.

On the first day the groove depth has no influence on the numbers of hMSCs bridges. However, on the third day the numbers of hMSCs bridges can be obviously influenced by groove depth when groove widths are 100  $\mu\text{m}$  ( $p < 0.01$ , One-way analysis of variance) or 50  $\mu\text{m}$  ( $p < 0.05$ , One-way analysis of variance). It suggests that hMSCs can simultaneously sense the depth and width of groove. Actually, two-way analysis of variance indicates that the interaction of groove depth and width dramatically influence the numbers of hMSCs bridges ( $p < 0.001$ ), on the third day. Attention must be paid to that only when the ratio of groove width to depth was less than two, cells can spanned across groove, otherwise no bridge would be observed on the third day (as a red boundary shown in table 2). Those phenomena may be related to the rigidity of cytoskeleton. Namely, cells prefer to span across barrier rather than bend themselves with too large angle when they meet different topography.<sup>38, 39</sup> Upon encountering a groove / ridge edge, the growth cone initiates filopodia to detect possible adhesion sites beyond the groove / ridge edge. If the ratio of groove width to depth is greater than or equal to two, it is more possible for filopodia to adhere to the top of one plateau or one side wall of groove and hMSCs extend between bottom and plateau or side wall as shown in Fig 2 A(a) and A(b). If the ratio of groove width to depth is less than two within the range of experiment testing, hMSCs chose to bridge across the groove avoiding bending themselves with large angle.

There is no statistical difference of the numbers of hMSCs of bridges between Day 1 and Day 3, though the average bridge numbers is larger on Day 3 than that on Day 1 to for most of experiment groups. Only the numbers of bridge on D100W100 ( $P < 0.05$ ) and D100W50 ( $P < 0.001$ ) signally increase from one day to three days. Maybe with the increasing of incubation time, the number of bridges composed of a few bunches of cells is raised, correspondingly the number of bridges composed of a bunch of cells decrease, resulting in none increase of the bridge numbers. Dramatically, the numbers of bridges on D25W50 and D50W100 decrease to zero on the third day. It proved once again that cells can perceive their microenvironment even the dimension of topography. Although hMSCs did cross the groove on the first day even when the ration of the width to depth is larger than or equal to two, they changed their choice when they had more time to sense the topography.

### The formation and keeping of hMSCs bridges

An unusual and surprising characteristic of the hMSCs observed in this study is that they have no underlying solid support while they span between two adjacent plateaus immersed in liquid media. Evelyn K.F.Yim<sup>38</sup> reported that neurites on plateaus initiates filopodia to detect grating depth. On deeper grating, when neurites encounter the plateaus edge, "either no filopodia could touch the bottom as they are not long enough or do not have a large enough tilt angle, or the neurite bending angle is too large,"<sup>38</sup> but the filopodia would touch the near plateaus and extend across grooves. In this study, the widths of grooves are too large for hMSCs filopodia on the plateaus to touch the near plateaus directly.

Observation of hMSCs by SEM provides initial insight into a potential mechanism by which the bridges could form. In some instances, hMSCs extended between the side wall and groove bottom (figure 2 A(a), C(a) and figure 3). We hypothesize that this lifting is an early event in the formation of a bridge. When cells at the groove bottoms perpendicularly met the groove walls, cells exerted forces on each other that overrode the effects of substrate features on hMSCs alignment and first adhered at both side walls of the groove, then lifted cells soma from the groove bottom and spanned across the groove. This result is consistent with Diane Hoffman-Kim's report.<sup>19</sup>

According to our results, hMSCs hanging above the groove were stable even when they were treated with 0.25  $\mu\text{g}/\text{ml}$  cytochalasin D or 1  $\mu\text{g}/\text{ml}$  nocodazole. After treated with cytochalasin or nocodazole, that hMSCs spanned above groove (D100W100, D100W50, D50W50, D50W25, D25W25) still could be observed by digital microscope. Cells use the actin edge-bundle (AEB) to maintain their spread shape on substrates.<sup>40</sup> It is a single curved microfilament bundle following the outline of every webbed edge of cells (figure 4).<sup>40-42</sup> Microtubules are not required to support the webbed edge.<sup>40</sup> So nocodazole did not destroy the hMSCs bridging. Furthermore, AEB is not usual stress fibers and appears more stable<sup>40</sup> in the presence of cytochalasin D treatment. So some hMSCs still spanned across grooves.

The average bridge numbers is larger on Day 3 than that on Day 1 to for most of experiment groups and the numbers of bridging increased with decreasing of drug (cytochalasin D and nocodazole) effect. It can be speculated that if the hMSCs bridging was disrupted, they would bridge again when they perpendicularly met the groove wall and the ratio of groove width to depth is less than two.

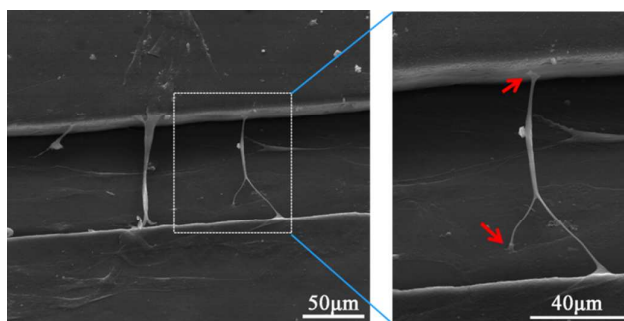


Figure 3. SEM pictures of hMSCs provide initial insight into a potential mechanism by which the bridges form. It is hypothesized that when cells at the groove bottoms perpendicularly met the groove walls, cells exerted forces on each other that could override the effects of substrate features on hMSCs alignment and adhered at both side walls of the groove, then lifted cells soma from the groove bottom and spanned across the groove.

### The properties of impending hMSCs

**The characterization of cytoskeletal** When cells spread on the plateaus or the groove bottoms, they exhibited a characteristic fibroblast-like phenotype with parallel actin stress fibers extending across the entire cytoplasm, as revealed by phalloidin-FITC staining (Figure 4). The actin stress fibers of cells, which spanned across the groove, were disorganized and actin edge-bundles were obvious as indicated by white arrows in figure 4. Focal adhesion can affect actin assembling and the structure of actin regulates the maturing of focal adhesion in return. The cells spanned across the groove as a filament with two apices anchoring at substrates with a large area of non-adhesion. The number of focal adhesions was too little to support for parallel actin stress fibers forming. The non-adhesive edge increased the membrane tension and further reinforced the stress fibers upon it.<sup>40-42</sup> When hMSCs spanned across the groove as a wide banding, F-actin aggregated upon the bridge edge, besides, parallel actin stress fibers were observed in the middle of bridge (figure 4 B1). Therefore, it can be inferred that when some cells extended across the groove together, they could touch and adhere to each other and shared the membrane tension caused by non-adhesion, then rebuilt their parallel actin stress fibers in the middle of bridge.

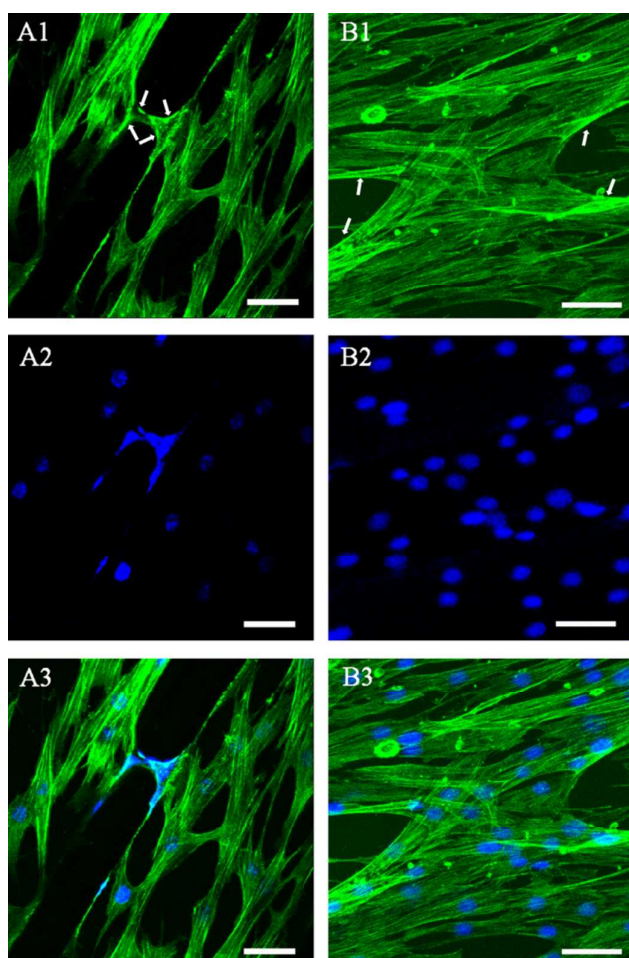


Figure 4. A1 and A2 were F-actin cytoskeleton (green) and cell nucleus (blue) labeled by FITC phalloidin and DAPI respectively in hMSCs cultured on micro-grooved PCL for 1 day. B1 and B2 were that cultured for 3 days. A3 and B3 were merged. The parallel actin stress fibers of bridging hMSCs were disorganized and the actin edge-bundles were very obvious (indicated by white arrow) (A1). When hMSCs spanned across the groove as a wide banding, F-actin aggregated upon the bridge edge but parallel actin stress fibers were observed in the middle of the bridge (B1). Scale bar = 50  $\mu\text{m}$ .

**The stiffness of impending hMSCs** Changes in cell-substrates interactions are usually associated with the expression of integrins and molecules in the FA plaque, which can influence F-actin organization and further cellular mechanical properties.<sup>43</sup> Studies suggest that cellular mechanical properties may serve as novel biological markers of cell phenotypes, reflecting changes in cell homeostasis, differentiation or transformation.<sup>26, 27, 44, 45</sup> AFM was used to test the elasticity modulus of hMSCs which spanned above different grooves (D100W100, D100W50, D50W50, D50W25, D25W25) and hMSCs spreading on flat substrate were used as control. Live cells are rather soft and delicate for AFM probing under physiological conditions. Besides, the groove and the bridging hMSCs are too narrow that make it is very difficult to measure the elasticity moduli of live bridging hMSCs accurately. Fixing with paraformaldehyde improves the AFM images and AFM indentation results. hMSCs were fixed by paraformaldehyde and dried in the air before measured by AFM in this study. Elasticity modulus of hMSCs are about 11~12 MPa in all groups (figure 5), besides, there is no difference between experimental groups and control group. Elasticity modulus of hMSCs measured in this study are much higher than that of live cells reported by other researchers (1.2~3.4 kPa)<sup>26, 46-49</sup>. The treatment of fixing solution or drying the samples in the air can increase the elasticity modulus value.<sup>50</sup> Although the F-actin disorganization is observed with laser confocal microscopy, the elasticity modulus shows no difference between bridging cells and normal spreading cells. Cells always reproduce their cytoskeleton architecture in response to cell-cell or cell-substrate contact.<sup>51</sup> The disorganized parallel actin stress fibers (figure 4 (A1)) captured by laser confocal microscopy may be temporary and will recover when more cells take part in the bridging (figure 4 (B1)).

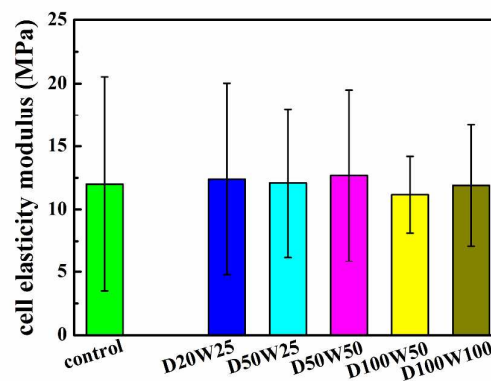


Figure 5. Elasticity modulus of hMSCs which spanned across grooves with different widths and depths or normally spread on flat PCL were tested by AFM. There was no difference between experiment groups and control, and among experiment groups.

**The protein express of bridging hMSCs** hMSCs can differentiate to osteoblasts, chondrocytes, adipocytes, neurocytes or myoblasts in different conditions. According to anatomy, cells in different tissue have different morphology and the morphology of hMSCs can also affect their fate and phenotypes.<sup>52-54</sup> Further researches indicate that focal adhesion influences cells morphology, cytoskeletal structure, traction force and signal path then to regulate cellular process, ranging from migration to differentiation.<sup>41, 42, 55</sup> When hMSCs spanned across the groove as a filament, their morphology was similar to myotube. However, desmin, which is the specific protein of myocyte, was not detected by immunofluorescence around the bridges (data not shown). Some bridging hMSCs presented skeleton structures which were similar to that of osteoblasts (figure 6). Beyond all expectations, osteocalcin was not expressed by them according to the immunofluorescence results (figure 6). Besides, results of ALP staining and alizarin red staining were also negative (data not shown). Mechanical signals regulate MSC osteogenic differentiation through Wnt/ $\beta$ -catenin,<sup>56, 57</sup> RhoA-ROCK<sup>58</sup> or Wnt5a and N-cadherin/ $\beta$ -catenin signaling pathway<sup>59</sup>. Related transcription factors such as Runx2 or  $\beta$ -catenin will be expressed, activated or increased in nuclear. The bridging hMSCs were not osteogenic differentiation. Runx2 would not be expressed, and the catenin is possible binding to cadherins in bridging hMSCs<sup>60</sup>. Maybe those bridging hMSCs were different from normal spread cells, but they were a small percentage of the cell population and influenced by others around them. On the other hand, cytoskeletal structures of bridging hMSCs are dynamic and always changing. Maybe there is not enough time and sufficient conditions for bridging hMSCs to osteogenic differentiate. Furthermote, detecting methods used in this study are crude and limited to test properties of bridging hMSCs. New experiments<sup>41</sup> and methods<sup>61</sup> will be used to further investigate those phenomena and the effect of this behavior of cells on their fate.

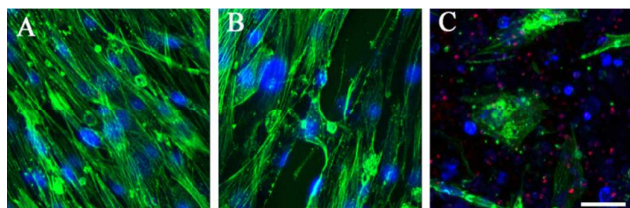


Figure 6. Osteocalcin staining of hMSCs after 21 days of culture. A, hMSCs were cultured on flat substrates with normal media as negative control. B, hMSCs were cultured on micro-grooved substrates as experiment group. C, hMSCs were cultured on 24 well plate with Osteogenesis induced media as positive control. Actin = green, DAPI = cell nucleus, Osteocalcin = red. Scale bar = 50  $\mu$ m.

## Conclusions

In addition to contact guidance, hMSCs in this study exhibited complex behaviors on the micro-grooved substrates, which contained a serial of grooves with different dimensions ranging from tens to hundreds of microns. A unique growth pattern that hMSCs spanned across grooves between adjacent plateaus was demonstrated and the widest groove which hMSCs could extend across was 100  $\mu$ m. hMSCs could not only percept the micron topography, but also sensed the ratio of width to depth of grooves. Only when the ratio of groove width to depth was smaller than two, hMSCs could span across the groove within the range of this testing. It is speculated that hMSCs on the bottom explored their possible adhesion positions and bridge across the groove by climbing side wall of groove. Furthermore, the parallel actin stress fibers were disorganized and actin edge-bundles were obvious when hMSCs spanned across groove. However, there was no difference between bridging hMSCs and normal spreading hMSCs on the result of cells elasticity modulus, expression of desmin and osteocalcin.

Owing to the multiple differentiation potential and low immunogenicity, hMSCs have attracted many researchers. It is vital to understanding the interaction and mechanism between hMSCs and their microenvironment for the purpose of directly inducing their differentiation. The results from this study can provide more information about the interaction between hMSCs and micron topography, and offer new concept for the design of future tissue engineering scaffold that tailor topographical features (i.e. pores) to optimize cell-scaffold interactions.

## Acknowledgements

This work was financially supported by the National Basic Research Program of China (Grant No. 2011CB606204 and 2012CB619100), the National Natural Science Foundation of China (Grant Nos. 51172073 and 51202069), and the Specialized Research Fund for the Doctoral Program of Higher Education of China (Grant No. 20110172120002).

## Notes and references

1. R. Jayakumar, M. Prabakaran, P. T. Sudheesh Kumar, S. V. Nair and H. Tamura, *Biotechnology advances*, 2011, **29**, 322-337.
2. D. Seliktar, *science*, 2012, **336**, 5.
3. S. Chen, L. Li, C. Zhao and J. Zheng, *Polymer*, 2010, **51**, 5283-5293.
4. H. Cui, M. J. Webber and S. I. Stupp, *Biopolymers*, 2010, **94**, 1-18.
5. H. Seyednejad, D. Gawlitta, R. V. Kuiper, A. de Bruin, C. F. van Nostrum, T. Vermonden, W. J. Dhert and W. E. Hennink, *Biomaterials*, 2012, **33**, 4309-4318.

6. T. Xu, K. W. Binder, M. Z. Albanna, D. Dice, W. Zhao, J. J. Yoo and A. Atala, *Biofabrication*, 2013, **5**, 015001.
7. R. Gauvin, Y. C. Chen, J. W. Lee, P. Soman, P. Zorlutuna, J. W. Nichol, H. Bae, S. Chen and A. Khademhosseini, *Biomaterials*, 2012, **33**, 3824-3834.
8. D. H. Kim, K. Han, K. Gupta, K. W. Kwon, K. Y. Suh and A. Levchenko, *Biomaterials*, 2009, **30**, 5433-5444.
9. M. Jamal, N. Bassik, J. H. Cho, C. L. Randall and D. H. Gracias, *Biomaterials*, 2010, **31**, 1683-1690.
10. R. Sorkin, T. Gabay, P. Blinder, D. Baranes, E. Ben-Jacob and Y. Hanein, *Journal of neural engineering*, 2006, **3**, 95-101.
11. P. C. Anna Webb, Jeremy Skepper, Alastair Compston and Andrew Wood, *Journal of Cell Science*, 1995, **108**, 2747-2760.
12. P. M. Stevenson and A. M. Donald, *Langmuir : the ACS journal of surfaces and colloids*, 2009, **25**, 367-376.
13. E. T. Baran, K. Tuzlakoglu, A. Salgado and R. L. Reis, *Journal of tissue engineering and regenerative medicine*, 2011, **5**, e108-114.
14. J. A. H. A. P. C. LETOURNEAU, *DEVELOPMENTAL BIOLOGY*, 1986, **117**, 655-662.
15. G. H. Kim and J. G. Son, *Applied Physics A*, 2008, **94**, 781-785.
16. D. Baranes, J. Cove, P. Blinder, B. Shany, H. Peretz and R. Vago, *Tissue engineering*, 2007, **13**, 473-482.
17. A. Leclerc, D. Tremblay, S. Hadjiantoniou, N. V. Bukoreshtliev, J. L. Rogowski, M. Godin and A. E. Pelling, *Biomaterials*, 2013, **34**, 8097-8104.
18. P. C. P. CLARK, A. S. G. CURTIS, J. A. T. DOW and C. D. W. WILKINSON, *Development*, 1990, **108**, 635-644.
19. J. S. Goldner, J. M. Bruder, G. Li, D. Gazzola and D. Hoffman-Kim, *Biomaterials*, 2006, **27**, 460-472.
20. H. Yang, L.-N. Gao, Y. An, C.-H. Hu, F. Jin, J. Zhou, Y. Jin and F.-M. Chen, *Biomaterials*, 2013, **34**, 7033-7047.
21. S. E. Bulman, V. Barron, C. M. Coleman and F. Barry, *Tissue Engineering Part B: Reviews*, 2013, **19**, 58-68.
22. Z.-y. Wang, E. Y. Teo, M. S. K. Chong, Q.-y. Zhang, J. Lim, Z.-y. Zhang, M.-h. Hong, E.-s. Thian, J. K. Y. Chan and S.-H. Teoh, *Tissue Engineering Part C: Methods*, 2013, **19**, 538-549.
23. S. Kumar, *Nat Mater*, 2014, **13**, 918-920.
24. J. H. Kim, X. Serra-Picamal, D. T. Tambe, E. H. Zhou, C. Y. Park, M. Sadati, J. A. Park, R. Krishnan, B. Gweon, E. Millet, J. P. Butler, X. Trepant and J. J. Fredberg, *Nat Mater*, 2013, **12**, 856-863.
25. I. Titushkin and M. Cho, *Biophys J*, 2007, **93**, 3693-3702.
26. I. A. T. a. M. R. Cho, *31st Annual International Conference of the IEEE EMBS*  
*Minneapolis, Minnesota, USA, September 2-6, , 2009*.
27. E. K. F. Yim, E. M. Darling, K. Kulangara, F. Guilak and K. W. Leong, *Biomaterials*, 2010, **31**, 1299-1306.
28. M. Labet and W. Thielemans, *Chemical Society reviews*, 2009, **38**, 3484-3504.
29. I. K. V. Ann-Christine Albertsson, *Advances in Polymer Science*, 2002, **157**, 1-32.
30. M. M. A. Jugminder S. Chawla, *International Journal of Pharmaceutics* 2002, **249**, 127-138.
31. R. R. R. CHANDRA, *Prog. Polym. Sci.*, 1998, **23**, 1273-1335.
32. R. Olivares-Navarrete, S. L. Hyzy, J. H. Park, G. R. Dunn, D. A. Haithcock, C. E. Wasilewski, B. D. Boyan and Z. Schwartz, *Biomaterials*, 2011, **32**, 6399-6411.
33. B. Tian, J. Liu, T. Dvir, L. Jin, J. H. Tsui, Q. Qing, Z. Suo, R. Langer, D. S. Kohane and C. M. Lieber, *Nature Materials*, 2012, **11**, 986-994.
34. S. Watari, K. Hayashi, J. A. Wood, P. Russell, P. F. Nealey, C. J. Murphy and D. C. Genetos, *Biomaterials*, 2012, **33**, 128-136.
35. M. Bigerelle, S. Giljean and K. Anselme, *Acta Biomaterialia*, 2011, **7**, 3302-3311.
36. M.-H. Kim, M. Kino-oka, N. Maruyama, A. Saito, Y. Sawa and M. Taya, *Biomaterials*, 2010, **31**, 7666-7677.
37. H. Li, Y. S. Wong, F. Wen, K. W. Ng, G. K. L. Ng, S. S. Venkatraman, F. Y. C. Boey and L. P. Tan, *Macromolecular Bioscience*, 2013, **13**, 299-310.
38. J. S. Chua, C. P. Chng, A. A. Moe, J. Y. Tann, E. L. Goh, K. H. Chiam and E. K. Yim, *Biomaterials*, 2014, **35**, 7750-7761.
39. P. C. P. CLARK, A. S. G. CURTIS, J. A. T. DOW and C. D. W. WILKINSON, *Development*, 1987, **99**, 439-448.
40. M. S. Z. a. G. Albrecht-Buehler, *Cell motility and the cytoskeleton*, 1989, 195-211.
41. K. Mandal, I. Wang, E. Vitiello, L. A. Orellana and M. Bolland, *Nature communications*, 2014, **5**, 5749.
42. M. Thery, A. Pepin, E. Dressaire, Y. Chen and M. Bornens, *Cell motility and the cytoskeleton*, 2006, **63**, 341-355.
43. D. Docheva, D. Padula, C. Popov, W. Mutschler, H. Clausen-Schaumann and M. Schiekler, *Journal of Cellular and Molecular Medicine*, 2008, **12**, 537-552.
44. A. J. Engler, S. Sen, H. L. Sweeney and D. E. Discher, *Cell*, 2006, **126**, 677-689.
45. E. M. Darling, S. Zauscher, J. A. Block and F. Guilak, *Biophysical Journal*, 2007, **92**, 1784-1791.
46. H. Yu, C. Y. Tay, W. S. Leong, S. C. Tan, K. Liao and L. P. Tan, *Biochemical and biophysical research communications*, 2010, **393**, 150-155.
47. G. Yourek, M. A. Hussain and J. J. Mao, *ASAIO journal*, 2007, **53**, 219-228.
48. W. Pan, E. Petersen, N. Cai, G. Ma, J. Run Lee, Z. Feng, K. Liao and K. Leong, *Conference proceedings : ... Annual International Conference of the IEEE Engineering in Medicine and Biology Society. IEEE Engineering in Medicine and Biology Society. Annual Conference*, 2005, **5**, 4854-4857.
49. A. Tijore, F. Wen, C. R. Lam, C. Y. Tay and L. P. Tan, *PLoS one*, 2014, **9**, e113043.
50. N. I. N. A. A. Mozhanova, A. A. Bukharaev, *APPLIED SURFACE SCIENCE* 1999, **141**, 345-349.
51. B. M. Gumbiner, *Cell*, 1996, **84**, 345-357.
52. Z. Pan, C. Yan, R. Peng, Y. Zhao, Y. He and J. Ding, *Biomaterials*, 2012, **33**, 1730-1735.
53. X. Yao, R. Peng and J. Ding, *Advanced materials*, 2013, **25**, 5257-5286.
54. C. S. Chen, *Science*, 1997, **276**, 1425-1428.
55. H. Miyoshi and T. Adachi, *Tissue engineering. Part B, Reviews*, 2014, **20**, 609-627.
56. T. F. Day, X. Guo, L. Garrett-Beal and Y. Yang, *Developmental cell*, 2005, **8**, 739-750.
57. T. F. Day and Y. Yang, *The Journal of bone and joint surgery. American volume*, 2008, **90 Suppl 1**, 19-24.

## Journal Name

## ARTICLE

58. D. M. P. Rowena McBeath, Celeste M. Nelson,<sup>2</sup> Kiran Bhadriraju, and Christopher S. Chen, *Developmental cell*, 2004, **6**, 483-495.
59. E. J. Arnsdorf, P. Tummala and C. R. Jacobs, *PloS one*, 2009, **4**, e5388.
60. M. Perez-Moreno and E. Fuchs, *Developmental cell*, 2006, **11**, 601-612.
61. X. T. Zheng and C. M. Li, *Chemical Society reviews*, 2012, **41**, 2061-2071.